Electrons and holes in a 40 nm thick silicon slab at cryogenic temperatures

K. Takashina,[a] K. Nishiguchi, Y. Ono, A. Fujiwara, T. Fujisawa,[b] Y. Hirayama,[c] and K. Muraki

NTT Basic Research Laboratories, NTT Corporation, Atsugi-shi, Kanagawa 243-0198, Japan

(Received 11 December 2008; accepted 13 March 2009; published online 7 April 2009)

We demonstrate low temperature operation of an electron-hole bilayer device based on a 40 nm thick layer of silicon in which electrons and holes can be simultaneously induced and contacted independently. The device allows the application of bias between the electrons and holes enhancing controllability over density and confining potential. We confirm that drag measurements are possible with the structure. © *2009 American Institute of Physics*. [DOI: 10.1063/1.3112602]

Electron-hole bilayers in which a two-dimensional electron gas (2DEG) and a two-dimensional hole gas (2DHG) coexist in close proximity have received considerable interest over the past few decades owing to the possibility of their hosting a condensation of indirect dipolar excitons.[1] Experimental devices with separate electrical contacts to the two constituent layers are considered to be ideal for investigating the physics of such systems since they allow interlayer interactions to be probed directly through Coulomb drag.[2,3] Although there have been a number of demonstrations of such devices, reports on the resulting physics have been relatively few, presumably due to their limited controllability and reliability.

III-V compounds are usually thought to be the materials of choice since they permit band engineering and high mobility. However, in semiconductor physics, silicon has provided the forerunning insights into emergent phenomena on more than one occasion.[4] Recent experiments on silicon-on-insulator (SOI) based devices have shown that separately contacted electrons and holes can indeed be achieved in silicon, where the two carrier types are simultaneously generated on opposite sides of a single silicon layer and separately contacted through phosphorus (P) and boron (B) doped regions.[5] Very recently, a device with electrons and holes confined in a silicon layer as thin as 22 nm has been demonstrated at room temperature.[6] However, layers of silicon that are too thin require very large electric field, which in turn increases effects of interface roughness and localization at cryogenic temperatures[7,8] where excitonic effects might be expected.

In this letter, we present a separately contacted electron-hole bilayer device based on a 40 nm thick SOI layer operating at cryogenic temperatures. We demonstrate that the application of bias between the electrons and holes allows coexistence at smaller electric field, enhancing controllability over electron-hole density and confinement potential. We confirm that drag measurements are possible with the structure.

The device consists of a nominally 40 nm thick (d) SOI metal-oxide-semiconductor field-effect transistor [Fig. 1(a)] made on a separation-by-implantation-of-oxygen substrate as in previous work.[9–12] It has a polycrystalline silicon front gate with a SiO_2 gate insulator ($t_{FOX} \sim 81$ nm); the substrate is used as a back gate where the buried oxide ($t_{BOX} \sim 380$ nm) acts as the gate insulator. The device is shaped into a Hall-bar geometry with each electrode terminated by two types of Ohmic contacts [Fig. 1(b)].[7] The contact regions are thickened by around 30 nm by local oxidation of silicon to minimize adverse effects of a thin SOI and are implanted with either P or B to form contacts to electrons or holes, respectively.

Any pair of n-type (p-type) contacts can be used to operate the device as a standard field effect transistor [Fig. 1(b)]. Figure 2(a) shows the current passing through pairs of n- and p-contacts (I_e and I_h) under a bias voltage of 10 mV as a function of front gate voltage V_{FG} at the base temperature of a ^{3}He cryostat ($T \sim 250$ mK). When $V_{BG}=0$ V, I_e increases with V_{FG}, corresponding to electrons being generated at the Si/SiO_2 interface closer to the front gate. The p-contacts do not connect to the 2DEG due to the depletion regions formed at each junction between the 2DEG and the p-contacts. Similarly, with negative V_{FG}, the p-channel conducts while the n-channel does not.

To generate electrons and holes simultaneously, a back-gate bias (V_{BG}) needs to be applied. When positive V_{BG} is applied, a 2DEG is generated at the interface closer to the back gate and the n-channel conducts even at $V_{FG}=0$ V. As V_{FG} is made negative, the n-channel is pinched off before the p-channel starts to conduct. As V_{BG} is made more positive, however, the gap region where both channels are insulating shrinks and eventually, at $V_{BG}=60$ V, both channels become conducting at $V_{FG} \leq V_{FG}^{*}(=-11$ V) demonstrating coexistence of electrons and holes. Without quantum confinement, electrons and holes are generated at opposite interfaces when the electric field F in the well becomes sufficiently high that the valence band top at the front interface lines up with the conduction band bottom at the back interface, i.e., $Fd=E_G$ at the Fermi level E_F [Fig. 2(b)]. This condition is slightly

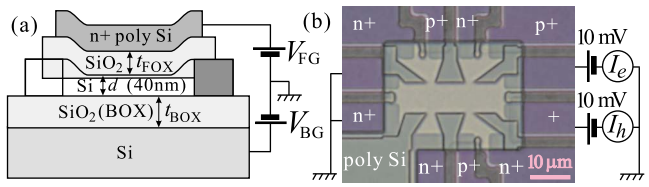

FIG. 1. (Color online) (a) Schematic diagram of a cross-section through the device. (b) Optical image of the Hall-bar device with a circuit diagram illustrating the setup for two-terminal measurements.

[a]Electronic mail: kei_t@nttbrl.jp.
[b]Present address: Tokyo Institute of Technology, Japan.
[c]Present address: Tohoku University and ERATO Nuclear Spin Electronics Project, Japan.

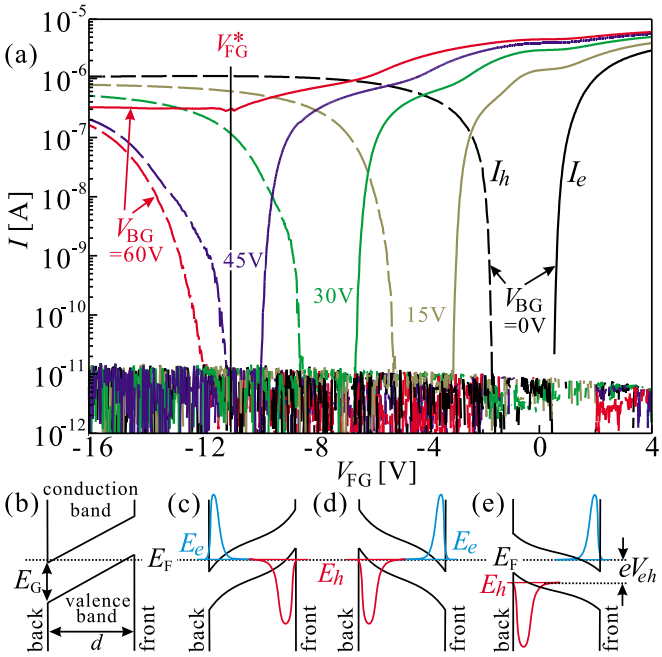

FIG. 2. (Color online) (a) Current through n- (I_e: solid lines) and p-contacts (I_h: dashed lines) at different V_{BG} taken with a bias of 10 mV. [(b) and (c)] Schematics of the potential required for coexistence without (b) and with (c) quantum confinement. (d) As (c) but with potential symmetrically reversed. (e) As (d) but with a bias (V_{eh}) applied to the 2D hole gas.

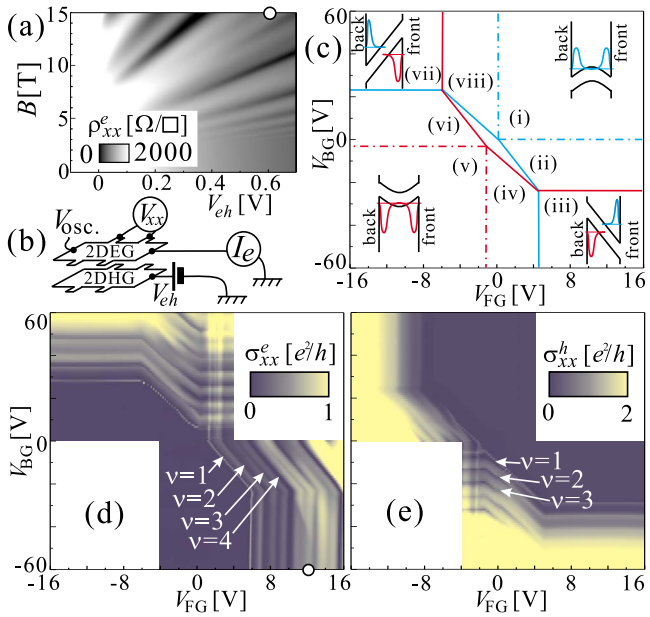

FIG. 3. (Color online) (a) Diagonal resistivity of the n-channel ρ_{xx}^e as functions of magnetic field B and interlayer bias V_{eh} applied through a p-contact with gate voltages fixed at V_{FG}=12 V and V_{BG}=−60 V. (b) Schematic diagram illustrating the setup used in (a). (c) Schematic diagram illustrating regions of the V_{FG}-V_{BG} plane with an interlayer bias of 0.6 V. Solid lines demarcate lines of zero electron (blue) and hole (red) density, while dashed lines indicate zero density of a second subband of a given carrier-type. The central diamond-shaped region bound by four solid lines corresponds to a situation where there are no carriers in the silicon slab. [(d) and (e)] Diagonal conductivity measured with n-channel contacts σ_{xx}^e and p-channel contacts σ_{xx}^h, respectively, at B=15 T, with an interlayer bias of 0.6 V. Identical points are marked by circles in (a) and (d).

modified when the quantum confinement is taken into account to E_h=E_F=E_e where E_h and E_e are the hole and electron subband edges, respectively [Fig. 2(c)]. The same conditions apply when the electric field is reversed by reversing the polarity of the gate voltages so that holes are generated at the back interface while electrons are at the front [Fig. 2(d)] (experimental data not shown).

Once electron-hole coexistence is achieved, the 2DEG or the 2DHG can be used as a gate for the other layer by applying an interlayer bias voltage V_{eh} which we define as the voltage applied to the 2DHG with respect to the chemical potential of the 2DEG [Fig. 2(e)]. Figure 3(a) shows Shubnikov–de Haas (SdH) oscillations of the 2DEG formed at the front interface with V_{FG}=12 V, V_{BG}=−60 V as a function of V_{eh} which is applied through a p-contact to the 2DHG [Fig. 3(b)]. The data clearly show a linear dependence of the carrier density on the interlayer bias reflecting the interlayer capacitance $C_{eh}\sim\epsilon/d_{eh}$. This in turn yields an effective interlayer separation d_{eh} between the electrons and holes of 30 nm using ϵ=11.9ϵ_0 as the dielectric constant where ϵ_0 is the permittivity of free space. We find the maximum interlayer bias, beyond which a significant interlayer current of above ~100 pA is seen, to be around 0.75 V independent of V_{FG} and V_{BG} under coexistence.

The spatial positions of the carriers within the silicon slab and their densities are determined by magnetotransport measurements as a function of V_{FG} and V_{BG}. Figures 3(d) and 3(e) show the longitudinal conductivity σ_{xx} converted from R_{xx} and R_{xy} measured with an interlayer bias of 0.6 V and a magnetic field of 15 T applied perpendicular to the 2D plane. SdH oscillations can be clearly seen for both electrons and holes. The Landau-level filling factors (ν) are determined from the Hall resistance measured simultaneously. The trajectories of the σ_{xx} minima in Figs. 3(d) and 3(e) identify the way in which electrons and holes are distributed in the well, which can be classified into eight regions [(i)–(viii)] in the V_{FG}-V_{BG} plane, as schematically shown in Fig. 3(c). When there is only one layer of 2DEG or 2DHG [(ii), (iv), (vi), and (viii)] the lines of constant-ν describe diagonal lines whose gradients are determined by the distances to the front and back gates.

When V_{BG} and V_{FG} are both large and of the same polarity [(i) or (v)], electrons (or holes) are generated at both interfaces and the SdH oscillations show a lattice pattern. The horizontal (vertical) lines represent the SdH oscillations of the carriers at the back (front) interface, which are relatively unaffected by V_{FG}(V_{BG}) due to the screening provided by the carriers at the front (back) interface. When V_{BG} and V_{FG} are both large and of the opposite polarity [(iii) and (vii)], electrons and holes are generated at opposite interfaces. In the magnetotransport, the onset of coexistence is manifested by the sudden change in the direction of the constant-ν trajectories from diagonal to horizontal or vertical; this occurs as a result of the existence of carriers at the opposite interface which screen the electric field from the gate behind, similar to the case in which there are two carrier layers of the same type [(i) and (v)]. Other than this screening effect, effects of the 2DHG on the 2DEG magnetotransport (and vice versa) are found to be rather weak, similar to the behavior observed with two carrier layers of the same type.

The densities of the carriers mapped out from the magnetotransport measurements as functions of V_{FG}, V_{BG}, and interlayer bias can be used to extrapolate the onset of carrier generation, which can then be compared with the threshold

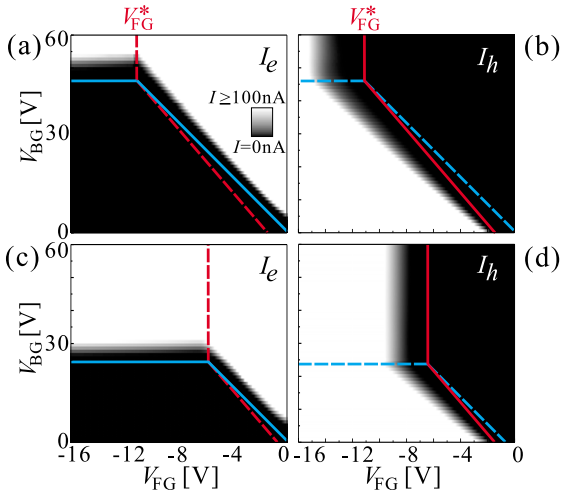

FIG. 4. (Color online) [(a) and (b)] I_e and I_h, respectively, with no interlayer bias. [(c) and (d)] I_e and I_h, respectively, with an interlayer bias of 0.6 V. Solid lines represent expected lines of zero carrier density for the carrier-type being measured while dashed lines correspond to the other carrier-type.

for conduction at zero magnetic field. In Figs. 4(a) and 4(b), we compare the expected lines of zero carrier densities and the current through the *n*- and *p*-channels in regions (vi)–(viii) without interlayer bias. Black regions between these lines and the threshold of conduction reflect insulating behavior or localization at low densities due to disorder. The data reveal that these regions grow as V_{FG} and V_{BG} become more asymmetric and the electric field F becomes stronger, reflecting the increasing effects of interface roughness. When an interlayer bias of 0.6 V is applied, the coexsistence region (vii) grows considerably and, at the same time, the localization region becomes narrower [Figs. 4(c) and 4(d)]. This occurs because the interlayer bias reduces the electric field in the well and hence the effects of interface roughness, demonstrating the additional control over the carrier properties provided by the interlayer bias.

Finally, for the demonstration of electron-hole drag, we perform the usual procedure of testing Onsager reciprocity and linearity [Fig. 5]. We choose a relatively high temperature of T=50 K where the signal can be expected to be reasonably large,[13] and V_{eh}=0 V where the measurement circuitry is simplest. A 2DHG of density $n_h \sim 5.2 \times 10^{15}$ m^{-2} is generated at the back interface with V_{BG}=−55 V. An AC (13.74 Hz) voltage of V_{osc}=10 mV is applied at the *n*-channel source electrode and in-phase and out-of-phase components of the drain current I_e and the longitudinal voltage along the *p*-channel V_h are recorded simultaneously as V_{FG} is swept (Fig. 5 inset). The in-phase signals are used to calculate the drag resistivity $\rho_{eh}=V_h/I_e(W/L)$ where W and L are the Hall-bar width and voltage-probe spacing as usual, while the out-of-phase signal is used to check for capacitive problems. We find that the sign of ρ_{eh} is positive, consistent with electrons and holes possessing opposite charge. Linearity is confirmed by measurements with

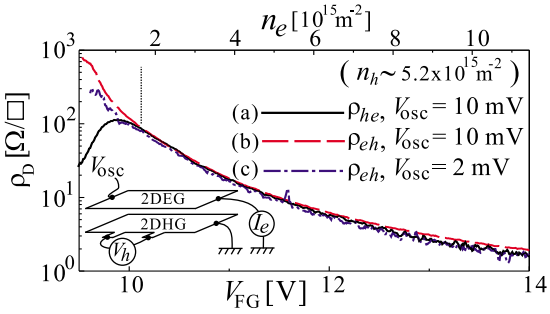

FIG. 5. (Color online) Electron-hole drag ρ_D at T=50 K, V_{BG}=−55 V. (a) $\rho_{he}=V_e/I_h(W/L)$. [(b) and (c)] $\rho_{eh}=V_h/I_e(W/L)$. ρ_{he} and ρ_{eh} agree well for $V_{FG}>10.1$ V marked by the vertical dotted line. Inset: Setting for measuring ρ_{eh}.

different V_{osc} [Figs. 5(b) and 5(c)]. Figure 5 also shows ρ_{he} (a) measured with the drive- and probe-layers interchanged (two exclusive sets of contacts). Above V_{FG}=10.1 V, ρ_{eh} and ρ_{he} agree rather well, showing the usual decrease with carrier density, confirming that the signal is indeed electron-hole drag in this range.

In conclusion, we have demonstrated a silicon-based separately contacted electron-hole bilayer device in which a bias can be applied between the electrons and holes allowing the confining potential to be controlled in addition to their densities. We anticipate that the device will allow extensive investigations into the physics of 2D electron-hole systems.

[1]Y. E. Lozovik and V. I. Yudson, JETP Lett. **22**, 556 (1975); S. I. Shevchenko, Sov. J. Low Temp. Phys. **2**, 251 (1976).
[2]U. Sivan, P. M. Solomon, and H. Shtrikman, Phys. Rev. Lett. **68**, 1196 (1992); S. Shapira, U. Sivan, P. M. Solomon, E. Buchstab, M. Tischler, and G. Ben Yoseph, *ibid.* **77**, 3181 (1996); M. Pohlt, M. Lynass, J. G. S. Lok, W. Dietsche, K. v. Klitzing, and K. Eberl, Appl. Phys. Lett. **80**, 2105 (2002); J. A. Keogh, K. Das Gupta, H. E. Beere, D. A. Ritchie, and M. Pepper, *ibid.* **87**, 202104 (2005); J. A. Seamons, D. R. Tibbetts, J. L. Reno, and M. P. Lilly, *ibid.* **90**, 052103 (2007).
[3]G. Vignale and A. H. MacDonald, Phys. Rev. Lett. **76**, 2786 (1996).
[4]K. v. Klitzing, G. Dorda, and M. Pepper, Phys. Rev. Lett. **45**, 494 (1980); S. Kravchenko, G. V. Kravchenko, J. E. Furneaux, V. M. Pudalov, and M. D'Iorio, Phys. Rev. B **50**, 8039 (1994); K. Hubner and W. Shockley, Phys. Rev. Lett. **4**, 504 (1960).
[5]K. Takashina, B. Gaillard, Y. Ono, and Y. Hirayama, Proceedings of the 2006 International Conference on Solid State Devices and Materials, Yokohama, 2006 (unpublished), pp. 830–831.
[6]M. Prunnila, S. J. Laakso, J. M. Kivioja, and J. Ahopelto, Appl. Phys. Lett. **93**, 112113 (2008).
[7]K. Takashina, B. Gaillard, Y. Ono, and Y. Hirayama, Jpn. J. Appl. Phys., Part 1 **46**, 2596 (2007).
[8]X. G. Feng, D. Popovic, and S. Washburn, Phys. Rev. Lett. **83**, 368 (1999).
[9]K. Takashina, A. Fujiwara, S. Horiguchi, Y. Takahashi, and Y. Hirayama, Phys. Rev. B **69**, 161304 (2004).
[10]K. Takashina, Y. Ono, A. Fujiwara, Y. Takahashi, and Y. Hirayama, Phys. Rev. Lett. **96**, 236801 (2006).
[11]K. Takashina, M. Brun, T. Ota, D. K. Maude, A. Fujiwara, Y. Ono, Y. Takahashi, and Y. Hirayama, Phys. Rev. Lett. **99**, 036803 (2007).
[12]Peak mobilities are around 0.2 and 0.8 m^2/Vs for holes and electrons, respectively.
[13]T. J. Gramila, J. P. Eisenstein, A. H. MacDonald, L. N. Pfeifer, and K. W. West, Phys. Rev. Lett. **66**, 1216 (1991).